

# Pixel Distillation: A New Knowledge Distillation Scheme for Low-Resolution Image Recognition

Guangyu Guo<sup>1</sup>, Longfei Han<sup>2</sup>, Junwei Han<sup>1</sup>, Dingwen Zhang<sup>1</sup>

<sup>1</sup>The Brain and Artificial Intelligence Laboratory, Northwestern Polytechnical University, Xi'an, China

<sup>2</sup>Beijing Technology and Business University, Beijing, China

<sup>1</sup>[https://nwpu-brainlab.gitee.io/index\\_en](https://nwpu-brainlab.gitee.io/index_en)

## Abstract

*The great success of deep learning is mainly due to the large-scale network architecture and the high-quality training data. However, it is still challenging to deploy recent deep models on portable devices with limited memory and imaging ability. Some existing works have engaged to compress the model via knowledge distillation. Unfortunately, these methods cannot deal with images with reduced image quality, such as the low-resolution (LR) images. To this end, we make a pioneering effort to distill helpful knowledge from a heavy network model learned from high-resolution (HR) images to a compact network model that will handle LR images, thus advancing the current knowledge distillation technique with the novel pixel distillation. To achieve this goal, we propose a Teacher-Assistant-Student (TAS) framework, which disentangles knowledge distillation into the model compression stage and the high resolution representation transfer stage. By equipping a novel Feature Super Resolution (FSR) module, our approach can learn lightweight network model that can achieve similar accuracy as the heavy teacher model but with much fewer parameters, faster inference speed, and lower-resolution inputs. Comprehensive experiments on three widely-used benchmarks, i.e., CUB-200-2011, PASCAL VOC 2007, and ImageNetSub, demonstrate the effectiveness of our approach.*

## 1. Introduction

Recently, great success has been made in many research fields of the computer vision community due to the large-scale deep neural networks. While current models, such as [6, 20, 50], have already achieved very promising performance in research, they are still hard to be readily equipped on edge computation devices, such as smartphones, embedded devices, small-size UAVs, etc. This is due to that these approaches are usually designed by complex network architectures and learn on large-scale high-quality training im-

ages. Unfortunately, the edge computation devices are limited in computational capacity and memory usage, and they might capture the naturally low-resolution images. When taking all these factors into account, current state-of-the-art deep models tend to be unusable.

To deal with this situation, knowledge distillation (KD) [16] techniques are received great attention in the past few years. In the existing knowledge distillation approaches, the student models are designed by using smaller network architectures than the teacher model—usually with fewer network layers or smaller channel dimension, thus reducing the requirement in floating point operations (FLOPs) and memory space. According to the current study, the two typical distillation schemes are the prediction-based distillation (PKD, see Fig. 1 (a)) and the feature-based distillation (FKD, see Fig. 1 (b)). Specifically, prediction-based distillation methods [2, 16, 29] utilize the soft prediction labels generated from the teacher model as the knowledge to guide the student model. In contrast, feature-based distillation methods [10, 33, 37, 46] utilize the intermediate features from different layers to transfer the semantic knowledge.

However, besides the internal network architecture, i.e., the depth and width of the deep model, the external factor, i.e., the input image resolution, reminds under-studied by the existing works. In fact, if the width and height of an image become  $K$  times smaller, the network would only require approximate  $1/K^2$  of the original FLOPs and running memory. In other words, compared with an original  $224 \times 224$  image, the model will save nearly 75% FLOPs and running memory if running on a  $112 \times 112$  image. Meanwhile, in many real-world applications, such as surveillance, the devices might be only equipped with low-resolution cameras to keep a low cost of memory storage. Under this circumstance, there is an urgent demand to enable the well-trained deep models to fit on LR images.

Based on the observations above, a new distillation framework, named pixel distillation is proposed (see Fig. 1 (c)). Compared with previous distillation frameworks, pixel distillation not only distills knowledge from the teacher net-

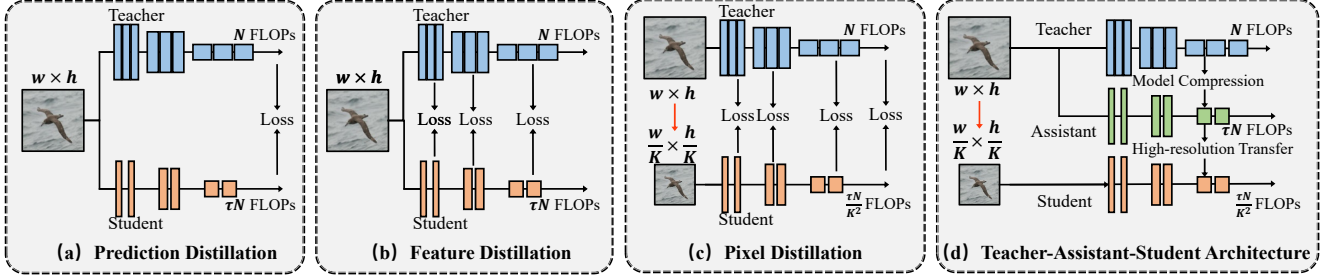


Figure 1. Illustrations of different knowledge distillation methods. (a-b) Previous prediction-based and feature-based knowledge distillation methods can reduce the computational cost by a factor of  $\tau$ . (c) Pixel distillation can further reduce the computational cost by using low-resolution input. (d) The proposed Teacher-assistant-student framework, which separates the pixel distillation process as a model compression stage and a high resolution representation transfer stage.

work’s features and predictions, but also distills knowledge from the network input resolution. The basic idea of our teacher-assistant-student (TAS) pixel distillation is shown in Fig. 2 (a). Specifically, we propose a two-stage distillation strategy to solve the pixel distillation problem. By introducing an assistant network into the classical Teacher-Student (TS) framework, we can reduce the performance degradation caused by both model compression and spatial resolution reduction. In the first stage, the aim of the assistant network is to hold useful knowledge from the teacher network when the network architecture becomes more compact. In the second stage, we adopt a high-resolution representation transfer (HRT) learning scheme to make the student network learn intermediate representation from the assistant network implicitly. Meanwhile, a high efficient feature super-resolution (FSR) module with LR inputs is designed to explicitly learn the HR feature maps, which can maintain more semantic-visual information (see in Fig. 2 (b)).

To summarize, the contribution of this paper is fourfold:

- We study a new distillation scheme, named pixel distillation, to learn efficient models with lightweight network architecture and low-resolution input.
- A novel Teacher-Assistance-Student distillation framework is established to unite the cross-resolution learning mechanism with the off-the-shelf knowledge distillation methods. Also, the high-resolution representation transfer learning and feature super-resolution module are designed to improve the performance of low-resolution input in implicit and explicit manner, respectively.
- Comprehensive experiments are conducted on three benchmarks to demonstrate the effectiveness and efficiency of the proposed distillation scheme.

## 2. Related Work

Hinton *et al.* first introduced the notion of knowledge distillation which aims to train a smaller model (*i.e.* student) via learning from the cumbersome models (*i.e.* teacher) [16]. The early knowledge distillation methods used the predicted score of the teacher model to guide the training of the student model. An essential way is to regard the predicted logits of the teacher model as the soft target of the student [2, 16]. Park *et al.* transfers mutual relations between different samples rather than the output of individual samples [29]. Yu *et al.* successfully applied knowledge distillation in metric learning [43].

Besides the predicted logits, many works have been proposed to guide the student by the intermediate representations of the teacher model [1, 4, 5, 14, 18, 24, 30, 34, 48, 53]. Compared with the logits, intermediate features is much more helpful to guide the student in more complex tasks, such as object detection [3], semantic segmentation [26] *etc.* The fundamental problem for distilling intermediate representations is that the dimension of the feature map is different between teacher and student network. Some of the previous works [14, 18, 33, 42] overcome these obstacles by building an adaptive module between hidden layers of teacher and student, which makes the student can not directly learn the intermediate representations. Besides that, Kim *et al.* proposed an unsupervised reconstruction method to align the dimension of factors used for distillation [17]. Similarity Preserving (SP) [37] unified the dimension in mini-batch level by matrix operation. DFA [10] introduced network architecture search [23] to learn the adaptive module between hidden layers of the teacher and student network. MFD [44] selected and matched the elements between the feature extracted from teacher network and it from student network to achieve knowledge distillation. On the other hand, some existing methods re-designed the loss function, including activation transfer loss with boundaries formed by hidden neurons [15], Jacobian [35], instance re-

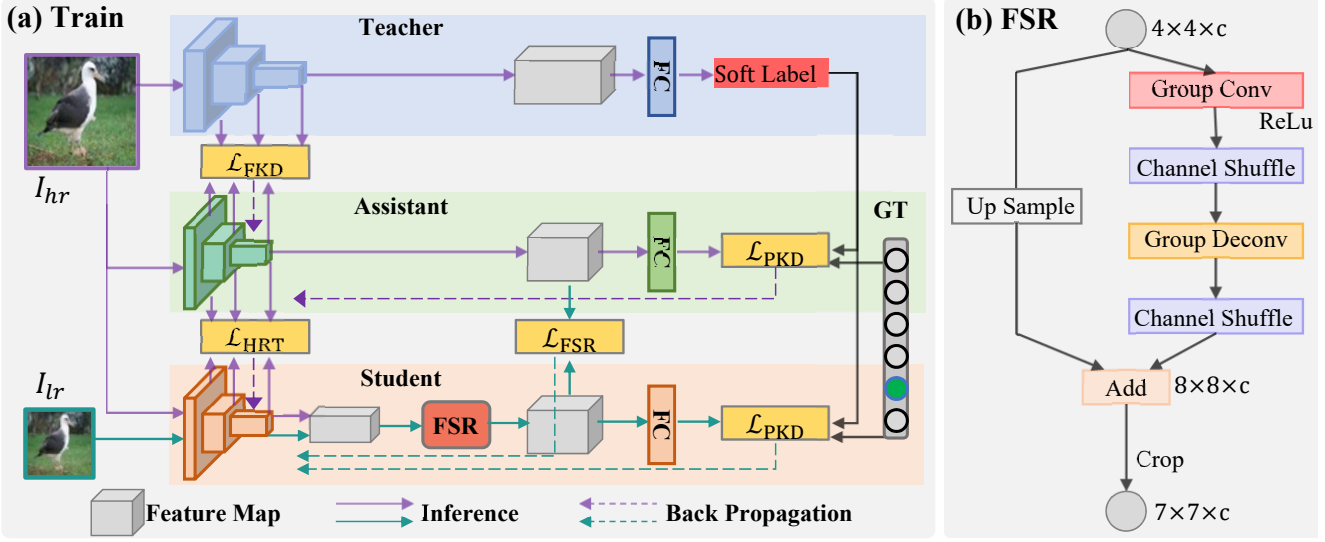


Figure 2. (a) Overview of the proposed method. The teacher is a cumbersome network pre-trained by high-resolution images. The student is a compact network that aims at working on low-resolution images. The assistant has the same network architecture as the student model, but use the same input size as the teacher model. (b) Network architecture for the feature super-resolution (FSR) module. Given a low-resolution feature maps with spatial size  $4 \times 4$ , the FSR module learns high-resolution feature maps with spatial size  $7 \times 7$ .

relationship graph [25], *etc.* Moreover, different works aim to minimize the similarity between the representation of the teacher and student network, Passalis *et al.* downsampled the teacher representation by t-SNE [28] and transfer probability to the student [30].

Knowledge distillation has been successfully applied to many tasks, like object detection [3, 21, 39, 41], semantic segmentation [26], *etc.* However, existing knowledge distillation approaches mainly dedicate on simplifying the structure of the model, lose sight of the input resolution which has a great relevance with the performance and computational cost. Moreover, due to the spatial resolution, the size of the intermediate feature maps is different between the teacher model and student model, some feature-based approaches can not be applied while the input spatial resolution are different.

### 3. Methods

In this paper, we aim to train a student model with the help of a teacher model, where both the network architectures and the input resolution are different. The teacher model takes high-resolution (HR) images as input and utilizes heavy networks, while the student model takes low-resolution (LR) images as input and utilizes a lightweight network.

#### 3.1. Preliminary Knowledge on KD

Traditional knowledge distillation approaches train a student network by learning the output from the teacher mod-

els. Based on the way to obtain the supervised information, we classify previous works into two categories, *i.e.*, prediction based methods and feature based methods. As shown in Fig. 1a, prediction based knowledge distillation methods train the student by using the class scores  $\mathbf{p}_t = \text{softmax}(\frac{\mathbf{x}_t}{T})$  predicted by the teacher:

$$\mathcal{L}_{\text{pkd}}(\mathbf{x}_t, \mathbf{x}_s) = (1 - \alpha)\mathcal{L}_{\text{cls}}(\mathbf{y}, \mathbf{x}_s) + \alpha T^2 \mathcal{L}_{\text{kl}}(\mathbf{p}_t, \mathbf{p}_s) \quad (1)$$

where  $\mathbf{y}$  is the ground truth,  $\mathbf{p}_s = \log(\text{softmax}(\frac{\mathbf{x}_s}{T}))$ ,  $\mathbf{x}_t$  and  $\mathbf{x}_s$  are the predicted class scores of the teacher and student model, respectively,  $T$  is a temperature parameter,  $\alpha$  is a hyperparameter to balance the classification loss  $L_{\text{cls}}$  and the Kullback–Leibler divergence loss  $L_{\text{kl}}$ .

Different from prediction based methods, feature based knowledge distillation methods further extract supervisions from the intermediate features of the teacher to guide the learning of the student:

$$\mathcal{L}_{\text{fkd}}(\mathcal{F}_t, \mathcal{F}_s, \mathbf{x}_s) = \mathcal{L}_{\text{cls}}(\mathbf{y}, \mathbf{x}_s) + \beta \delta \sum_{i=1}^M (g_t(\mathbf{F}_t(i)), g_s(\mathbf{F}_s(i))) \quad (2)$$

where  $\mathcal{F}_s = \{\mathbf{F}_s(1), \mathbf{F}_s(2), \dots, \mathbf{F}_s(M)\}$  and  $\mathcal{F}_t = \{\mathbf{F}_t(1), \mathbf{F}_t(2), \dots, \mathbf{F}_t(M)\}$  denote the features of teacher and student,  $M$  is the number of blocks in the network,  $g_t(\cdot)$  and  $g_s(\cdot)$  denote functions to extract information from intermediate features,  $\delta(\cdot)$  is the distance metric function,  $\beta$  is a hyperparameter to balance the classification loss and feature distillation loss.

### 3.2. TAS Framework for Pixel Distillation

As illustrated in Fig. 2 (a), to reduce the performance degradation caused by both the LR input and the compact architecture in pixel distillation, we introduce an assistant network into the classical teacher-student framework. The assistant network utilizes the same input resolution as the teacher model and maintains the same network architecture with the student. Compared to the traditional teacher-student structure, the proposed teacher-assistant-student framework can bring the following advantages for pixel distillation: 1) No resolution difference exists between the teacher model and the assistant model. Under this circumstance, any off-the-shelf knowledge distillation methods can be directly used here. In contrast, if we use the conventional teacher-student framework here, some knowledge distillation methods can not be used as they require features from the teacher and student have the same spatial resolution [17, 46]. 2) When the assistant network and student network utilize the same input resolution, feature maps from them will have the same dimension, whether the spatial resolution or the number of channels, which makes it easier and more efficient for the student to learn from HR images.

In fact, the assistant network disentangles the learning process into two stages. In the first stage, the assistant network  $f_a(\mathbf{W}_a, \cdot)$  is trained by learning the representation provided by the teacher  $f_t(\mathbf{W}_t, \cdot)$ , where  $f_t(\cdot)$  and  $f_a(\cdot)$  denote the network inference operation,  $\mathbf{W}_t$  and  $\mathbf{W}_a$  denote the trainable weights. This is a standard knowledge distillation problem and we can directly utilize one off-the-shelf knowledge distillation method here to reduce the performance degradation caused by the compact network architecture. In this stage, both the teacher model and the assistant model take high-resolution image  $I_{hr}$  as inputs. The loss of the assistant model  $\mathcal{L}_a$  could be either Eq 2 or Eq 3, according to the designs in the framework.

In the second stage, the student network  $f_s(\mathbf{W}_s, \cdot)$  is learned under the guidance of the assistant network. As shown in Fig. 2 (a), there are two settings in each training iteration of the student model: One is the implicit training setting, in which the student network uses the same high-resolution input images as the assistant network. In this training setting, we propose a high-resolution representation transfer (HRT) learning scheme to let the student network mimic the intermediate features from the assistant network. Since the student model has the same network architecture as the assistant model, it should produce the same intermediate representation as the assistant when using the high-resolution images as input. Under this circumstance, we use the  $L_2$  loss to guide the intermediate features of the

student model:

$$\mathcal{L}_{hrt}(\mathcal{F}_a, \mathcal{F}_s^{im}) = \sum_{i=1}^M \frac{1}{N(i)} \| \mathbf{F}_a(i) - \mathbf{F}_s^{im}(i) \|_2^2 \quad (3)$$

where  $\mathcal{F}_a = \{\mathbf{F}_a(1), \mathbf{F}_a(2), \dots, \mathbf{F}_a(M)\}$  is the intermediate features of the assistant model,  $\mathcal{F}_s^{im} = \{\mathbf{F}_s^{im}(1), \mathbf{F}_s^{im}(2), \dots, \mathbf{F}_s^{im}(M)\}$  is the intermediate features of the student model in this explicit phrase,  $N^i$  is the number of elements for the  $i$ -th feature. The loss of the implicit training phrase is:

$$\mathcal{L}_{s,im} = \mathcal{L}_{pkd}(\mathbf{x}_t, \mathbf{x}_s^{im}) + \eta \mathcal{L}_{hrt}(\mathcal{F}_a, \mathcal{F}_s^{im}), \quad (4)$$

where  $\mathbf{x}_{s,im}$  is the predicted classification scores in the implicit learning phrase.

Different from the implicit training setting, the student network would be directly trained with the LR images as the inputs in the explicit training setting. This training setting would enable the network model to perform well on LR inputs explicitly. To achieve this goal, a novel feature super-resolution (FSR) module is introduced here to explicitly reduce the performance gap caused by the LR inputs (details of the FSR module is provided in Section 3.3). The loss for this explicit training setting is defined as:

$$\mathcal{L}_{s,ex} = \mathcal{L}_{pkd}(\mathbf{x}_t, \mathbf{x}_s^{ex}) + \gamma \mathcal{L}_{fsr}. \quad (5)$$

Finally, the loss of the student network is the sum of these two training settings:

$$\mathcal{L}_s = \mathcal{L}_s^{im} + \mathcal{L}_s^{ex} \quad (6)$$

### 3.3. Feature Super-Resolution

Even though the proposed high-resolution representation transfer learning scheme can provide intermediate supervision to the student network, its learning process is still not straightforward as the low-resolution input is not used in the training process of the student model. To explicitly mitigate the performance gap caused by the difference of input resolution, we propose a feature super-resolution (FSR) module to enable the student model to learn a better feature representation for classification. The FSR module is inspired by the success of previous image super-resolution methods in reconstructing high-resolution (HR) nature images from low-resolution (LR) images [19, 22]. In the conventional image super-resolution task, the super-resolution (SR) model can be described as

$$I_{hr} = f_{sr}(\mathbf{W}_{sr}, I_{lr}), \quad (7)$$

where  $f_{sr}(\cdot)$  and  $\mathbf{W}_{sr}$  denote the network inference operation and trainable weights of the SR model. In our proposed methods, we have the high-resolution feature maps

Table 1. The configuration of teacher and student networks. 'Params' denotes the number of parameters.

			(a)	(b)	(c)	(d)
Teacher	Backbone		ResNet101	ResNet101	ResNet50	ResNet50
	Size 224 <sup>2</sup>	Params (M)	44.55	44.55	25.56	25.56
		FLOPs (M)	15667.94	15667.94	8223.03	8223.03
Student	Backbone		ResNet50	ResNet18	ResNet18	ShuffleNetV2 1.0
	Compression type		Depth	Depth & channel	Depth & channel	Different architecture
	K=2	Params (M)	28.84	11.89	11.89	2.31
	Size 112 <sup>2</sup>	FLOPs (G)	2476.61	993.22	993.22	86.94
		Efficient Ratio	84.2%	93.7%	87.9%	98.9%
	K=4	Params (M)	32.11	12.10	12.10	2.33
	Size 56 <sup>2</sup>	FLOPs (M)	987.90	284.78	284.78	29.45
	Efficient Ratio	93.7%	98.2%	96.5%	99.6%	

extracted by the assistant network, *i.e.*,  $\mathcal{F}_{hr} = \mathcal{F}_a$ . The low-resolution feature maps  $\mathcal{F}_{lr} = \{\mathbf{F}_{lr}(1), \mathbf{F}_{lr}(2), \dots, \mathbf{F}_{lr}(M)\}$  and predicted classification scores  $\mathbf{x}_s^{ex}$  are extracted from the student model with low-resolution input:

$$\{\mathcal{F}_{lr}, \mathbf{x}_s^{ex}\} = f_s(\mathbf{W}_s, I_{lr}). \quad (8)$$

As using the FSR module after a middle layer of a neural network will greatly increase the computational cost of the subsequent layers, in this work, we add the FSR module after the final convolution layer. Then, the low-resolution feature maps  $\mathbf{F}_{lr}(M)$  strive to approach the high-resolution feature maps  $\mathbf{F}_{hr}(M)$  via the proposed FSR module:

$$\widehat{\mathbf{F}}_{hr}(M) = f_{fsr}(\mathbf{W}_{fsr}, \mathbf{F}_{lr}(M)), \quad (9)$$

where  $f_{fsr}$  and  $\mathbf{W}_{fsr}$  is the network inference operation and trainable weights of the FSR module,  $\widehat{\mathbf{F}}_{hr}^M$  is the predicted feature map of FSR. We utilize  $L_2$  loss to train the FSR module as follows:

$$\mathcal{L}_{fsr} = \frac{1}{N \times M} \|\mathbf{F}_{hr}(M) - \widehat{\mathbf{F}}_{hr}(M)\|_2^2, \quad (10)$$

where  $N \times M$  indicates the number of elements in the feature map. The loss two classification branch are trained by the classification loss.

The detailed architecture of our FSR module is shown in Fig. 2 (b). An FSR module consists of several residual blocks (up to 2 in this work). For a single block, we first transfer the up-sample it by a factor of 2 in spatial resolution in one branch. Then, the residual between the target feature map and the up-sampled feature map are learned in another branch. Finally, we add the residual and up-sampled feature map together, formulating new feature representation. To reduce the computation cost and the number of parameters, we use group convolution, group deconvolution and channel shuffle in our FSR module [49]. Notice that crop is used if necessary to match the spatial size of the target feature map (e.g. from  $8 \times 8$  to  $7 \times 7$ ).

Improving the spatial resolution of the final layer would bring two benefits. First, it helps to improve the classification performance of the student network, as the learned high-resolution feature map contains more semantic information. Second, the high-resolution feature map makes it is possible to implement many previous image recognition algorithms under small input resolution. Many image recognition methods use class activation maps (CAM) [51] or feature maps of the last block to mine the location and appearance information [11, 40, 52]. However, for ResNet18 with input size  $56 \times 56$ , the spatial resolution of the last feature map as well as CAM is only  $2 \times 2$ , which contains little spatial and visual information. By using the FSR module, we can get feature maps and CAM of spatial resolution  $7 \times 7$  which contains richer location and appearance information.

## 4. Experiments

### 4.1. Settings

**Datasets.** We conduct experiments on three widely used datasets, *i.e.*, CUB (Caltech-UCSD Birds-200-2011) [38], VOC07 (PASCAL VOC 2007) [9], and ImageNetSub [32]. VOC07 is a multi-label dataset which covers 20 common categories and contains 2501, 2510, and 4952 images in train, validation, and test subset, respectively. We train our model on the trainval subset and evaluate the performance on the test subset. CUB is a fine grained dataset which consists of 200 categories of birds, there are 5994 training images and 5794 testing images. Same as [32], ImageNetSub uses the first 100 categories of the large-scale classification dataset ImageNet [8], with approximately 1300 training and 50 validation images per category. In total, it contains 129395 and 5000 images for train and validation, respectively.

**Metrics.** For evaluating the classification performance, we use mean average precision (mAP) for VOC07, and Top-1 accuracy (ACC) for CUB and ImageNetSub. To compare the computational cost of different models, we report the

Table 2. Results of ResNet series on VOC07 and CUB. "TS" denotes the teacher-student framework, and "TAS" denotes the proposed teacher-assistant-student framework. † indicates the original AT can not be used when the input resolution is different, we use average pooling to align feature maps following [36]. blue text denotes the performance is lower than the vanilla model, red text means how much our method outperforms the baseline knowledge distillation methods.

		K=2			K=4		
		(a)	(b)	(c)	(a)	(b)	(c)
VOC07	Teacher	91.29	91.29	90.74	91.29	91.29	90.74
	Student	82.21	76.55	76.55	60.36	56.58	56.58
	KD (TS) [16]	84.64	79.56	79.74	71.17	65.77	65.38
	+Ours (TAS)	86.53 <sup>+1.89</sup>	81.93 <sup>+2.37</sup>	81.51 <sup>+1.77</sup>	74.63 <sup>+3.46</sup>	70.07 <sup>+4.30</sup>	69.99 <sup>+4.61</sup>
	AT (TS) [46] <sup>†</sup>	79.23	71.91	73.1	38.29	39.28	41.76
	+Ours (TAS)	86.07 <sup>+6.84</sup>	81.29 <sup>+9.38</sup>	81.39 <sup>+8.29</sup>	74.67 <sup>+36.38</sup>	69.45 <sup>+30.17</sup>	69.97 <sup>+28.21</sup>
	SP (TS) [37]	85.11	79.43	79.72	67.86	62.41	64.09
	+Ours (TAS)	86.76 <sup>+1.65</sup>	82.69 <sup>+3.26</sup>	82.25 <sup>+2.53</sup>	75.12 <sup>+7.26</sup>	70.45 <sup>+8.04</sup>	70.46 <sup>+6.37</sup>
CUB	Teacher	71.52	71.52	71.81	71.52	71.52	71.81
	Student	53.15	42.94	42.94	25.08	19.6	19.6
	KD (TS) [16]	54.72	46.90	47.13	30.11	26.46	26.18
	+Ours (TAS)	60.83 <sup>+6.11</sup>	54.79 <sup>+7.89</sup>	54.25 <sup>+7.12</sup>	34.85 <sup>+4.74</sup>	30.51 <sup>+4.05</sup>	31.18 <sup>+5.00</sup>
	AT (TS) [46] <sup>†</sup>	53.94	45.70	44.21	12.13	17.85	16.22
	+Ours (TAS)	62.71 <sup>+8.77</sup>	55.31 <sup>+9.61</sup>	55.34 <sup>+11.13</sup>	36.49 <sup>+24.36</sup>	32.37 <sup>+14.52</sup>	31.66 <sup>+15.44</sup>
	SP (TS) [37]	50.60	44.48	42.39	11.08	16.47	18.57
	+Ours (TAS)	60.19 <sup>+9.59</sup>	53.89 <sup>+9.41</sup>	53.97 <sup>+11.58</sup>	35.32 <sup>+24.24</sup>	30.50 <sup>+14.03</sup>	30.70 <sup>+12.13</sup>

FLOPs (floating point operations) and number of parameters for all the models used in our work. We also propose a metric, named "Efficient Ratio", to evaluate the reduction of the computational costs, which is calculated as:

$$\text{Efficient Ratio} = 1 - \frac{\text{FLOPs (Student)}}{\text{FLOPs (Teacher)}}. \quad (11)$$

**Teacher-student pairs** The experimental results of knowledge distillation methods are usually evaluated on various teacher-student pairs. In Table 1, we provide the detailed setting of four teacher-student pairs with two down-sampling rate, including the model size (Params), computational cost (FLOPs), compression type and efficient ratio. Different from previous knowledge distillation works, Wide Residual Network [45] is not used because in the proposed pixel-distillation the teacher networks are trained by high-resolution images. Majority of our experiments, *i.e.* (a)-(c), use variants of ResNet [13] architectures as the teacher and student networks. We also introduce ShuffleNetV2 1.0 [27] in setting (d) to explore the generalization with different types of architectures.

**Implementation details.** In this paper, the spatial size of high-resolution input is  $224 \times 224$ , we use two down-sampling rate, *i.e.*  $K = 2$  and  $K = 4$ , so the spatial size of low-resolution input is  $\frac{224}{K} \times \frac{224}{K}$ . We use mini-batch stochastic gradient descent (SGD) as the optimizer, the momentum and the weight decay is set as 0.9 and 0.0005, re-

spectively. On VOC07 and CUB, we train the model by 45 epochs with batch size 32. When student build on the ResNet variants, we set the learning rate as 0.001 in the first 30 epochs and then reduced by a factor of 10 for the remaining 15 epochs. For the setting (d) built on ShuffleNetV2 1.0, we modify the learning rate as 0.01, and follow the same setting as the ResNet. We set  $\gamma = 14$  and  $\eta = 1.5$ , the number of groups in FSR is set 32 for ResNet and 1024 for ShuffleNetV2 1.0, detailed experiments are provided in the supplement. Our code is implemented on the basis of PyTorch [31], and all experiments are running on a Tesla V100S GPU.

## 4.2. Experimental Results

**VOC07 and CUB.** We try three knowledge distillation methods in the first stage of our framework, *i.e.* prediction distillation method KD [16], and feature distillation method AT [46], SP [37]. AT [46] is selected as a representative of methods requiring the same spatial resolution for features from teacher and student, we use average pooling to align feature maps following [36]. SP [37] is a representative of methods that do not need the features of teacher and student to have the same spatial resolution, which can be directly used to resolve the pixel distillation problem. In Table 2, KD [16], AT [46] and SP [37] indicate that we directly utilize these methods with classical teacher-student framework, while "+Ours" indicate these methods are used

Table 3. Experimental results of setting (d) whose teacher and student belong to different types of network architecture. **blue** text denotes the performance is lower than the vanilla model, **red** text means how much our method outperforms the baseline knowledge distillation methods, and the meaning of the **green** text is opposite to that of the **red**.

		Teacher	Student	KD [16]	+Ours	AT [46] <sup>†</sup>	+Ours	SP [37]	+Ours
VOC07	K=2	90.74	71.81	66.55	75.24 <sup>+8.69</sup>	38.96	75.42 <sup>+36.46</sup>	36.13	75.71 <sup>+39.58</sup>
	K=4	90.74	58.91	56.35	62.08 <sup>+5.73</sup>	32.86	62.04 <sup>+29.18</sup>	30.25	62.18 <sup>+31.93</sup>
CUB	K=2	71.81	45.35	43.54	45.83 <sup>+2.29</sup>	21.49	48.15 <sup>+26.69</sup>	2.86	40.69 <sup>+37.83</sup>
	K=4	71.81	25.78	25.27	24.57 <sup>-0.70</sup>	4.45	26.16 <sup>+21.71</sup>	1.60	20.92 <sup>+19.32</sup>

between the teacher network and assistant network. Since the original AT [46] can not be used when the input resolution is different, we use average pooling to align feature maps following [36]. Following [24, 36], we set  $\alpha = 0.9$ ,  $T = 4$  for the prediction distillation loss, and set  $\beta$  as 1000 and 3000 for AT [46] and SP [37], respectively.

In Table 2 we provide the experiment results of ResNet variants, *i.e.* setting (a)-(c). For these three knowledge distillation baseline methods, we can observe that both KD can stably obtain performance gains compared to the vanilla students, but two feature-based methods may collapse under some circumstances. To be specific, AT only obtains performance gains on CUB when the down-sampling rate is 2. performs well on the VOC07 but fails on the CUB dataset. The reason of this phenomenon is that a higher down-sampling rate will lead to a larger gap between the input space of the teacher network and the student network. It has been proven that knowledge distillation struggles when the student network is too weak to successfully mimic the teacher network [7], if the gap between the teacher and student is too large.

Moreover, results in Table 2 show that the proposed method can stably increase the performance compared to the vanilla network. Further on, our method can stably improve the performance compared with three baseline methods, which demonstrates that the proposed assistant network is effective to utilize the previous knowledge distillation methods in our AST framework by decoupling model compression and resolution reduction. Especially, based on the proposed method, ResNet18 outperforms the vanilla ResNet50 when the resolution of input image is  $112 \times 112$  (82.69 vs. 82.21 on VOC07, 54.79 vs. 53.15 on CUB), while alleviating 54.2% computational cost (0.99G vs. 2.17G in terms of FLOPs).

Table 3 provides the results of setting (d) where the teacher and student are built with different types of architecture, we can observe that both three baseline methods and our methods fail to stably improve the performance compared to the vanilla network, especially when the down-sampling rate is 4. This is caused by the enlarged gap between the teacher and student network when using different architectures, which makes it hard for the student network to learn useful information from the teacher network.

Meanwhile, experiments in [36]<sup>1</sup> also indicate that the traditional knowledge distillation methods may collapse when the teacher and student have different architectural types.

**Experiments on ImageNetSub** For experiments on the ImageNetSub, we use KD [16] as the baseline as experiments in VOC07 and CUB have proven its stability on the pixel distillation problem. We train models 90 epochs with batch size 256, the learning rate is 0.1 reduced by a factor of 10 in 30 and 60 epochs, others parameters are kept the same as the VOC and CUB. Table 4 provides the results of setting (a)-(c) for down-sampling rates 2 and 4, we can observe that our proposed methods can stably outperform KD in all 6 experiments. To be specific, for setting (b) with down-sampling rate 2, our method outperforms KD by 2.84 (65.88 vs. 63.04), and ResNet18 trained by our method obtains 11.14 performance gains than the vanilla ResNet18 (65.88 vs. 54.74).

Table 4. Results of ResNet series on ImageNetSub. **red** text means how much our method outperforms the baseline knowledge distillation methods.

		(a)	(b)	(c)
Teacher		72.34	72.34	70.44
Student		61.80	54.74	54.74
K=2	KD (TS) [16]	65.90	63.04	63.16
	+Ours (TAS)	66.56 <sup>+0.66</sup>	65.88 <sup>+2.84</sup>	64.48 <sup>+1.32</sup>
Student		47.92	43.08	43.08
K=4	KD (TS) [16]	51.18	50.04	49.95
	+Ours (TAS)	51.98 <sup>+0.80</sup>	51.16 <sup>+1.12</sup>	51.02 <sup>+1.07</sup>

### 4.3. Model Analysis

**Ablation study of the key learning components.** As shown in Table 5, we conducted our ablation study on the VOC07 and CUB. In the ablation study, the teacher network is built on ResNet101 with input resolution  $224 \times 224$ , and the student network is ResNet18 with input resolution  $56 \times 56$ , baseline denotes the vanilla ResNet18 trained with input resolution  $56 \times 56$ . The experiment results on the

<sup>1</sup><https://github.com/HobbitLong/RepDistiller>

Table 5. Ablation study of components in the proposed methods. Experiments are conducted on VOC07 and CUB. † denotes model are trained by the proposed TAS framework.

	✓	✓	✓	✓
Baseline	✓	✓	✓	✓
KD [16]		✓	✓	✓
FSR†			✓	✓
HRT†				✓
VOC07	56.58	65.77	69.14	70.07
CUB	19.60	26.46	29.95	30.51

VOC07 dataset show that the performance will improve from 56.58 to 65.77 via directly using traditional knowledge distillation (KD) [16] approach. Then, by integrating KD and our proposed FSR module in the proposed teacher-assistant-student framework, we can get 3.37 performance gains. Finally, we can get an mAP of 70.07 after the proposed HRT learning, which is 13.49 higher than the baseline. Such notable performance gain demonstrates that our proposed learning framework can work effectively with lightweight network architecture and small input resolution.

**Analysis of the TAS framework.** In Table 6, we apply the proposed TAS framework to previous knowledge distillation methods to explore the importance of the TAS framework for the pixel distillation problem. To be specific, KD with TS means we use KD one time between teacher and student, KD with TAS means KD is used two times, *i.e.* between teacher-assistant and assistant-student. From the results, we can observe that only KD can achieve a slight performance gain than TS when using the TAS framework. This is because previous knowledge distillation methods mainly focus on the model compression problem and can not deal with the problem of resolution reduction. The performance of the assistant network also can prove this conclusion: both three baseline methods can obtain high performance to the assistant network when the input resolution is unchanged. Also, the results of Table 6 demonstrate that our proposed HRT learning scheme and the FSR module can better deal with the problem of resolution reduction than the previous knowledge distillation methods.

**Ablation studies about hyperparameter  $\gamma$  and  $\eta$ .**  $\gamma$  and  $\eta$  are the loss weights of the proposed FSR module and HRT learning, respectively. In Fig. 3, we conduct experiments on the baseline with FSR module to analyze how  $\gamma$  effect the performance of the FSR module, where the teacher network is ResNet101 with input resolution  $224 \times 224$ , and the student network is ResNet18 with input resolution  $56 \times 56$ . As shown in Fig. 3a and Fig. 3b, we can observe that the performance is not sensitive to loss weight  $\eta$  and  $\gamma$  as the performance fluctuates within 0.6 for different values. This is because both FSR and the HRT learning are not only trained by features from the assistant

Table 6. Effectiveness analysis of the proposed TAS framework.

Teacher	91.29	Vanilla	56.58
Methods	Framework	Assistant	Student
KD	TS	-	65.77
KD	TAS	87.77	66.26
KD+Ours	TAS	87.77	<b>70.07</b>
AT	TS	-	39.28
AT	TAS	84.91	32.89
AT+Ours	TAS	84.91	<b>69.45</b>
SP	TS	-	62.41
SP	TAS	87.91	56.19
SP+Ours	TAS	87.91	<b>70.45</b>

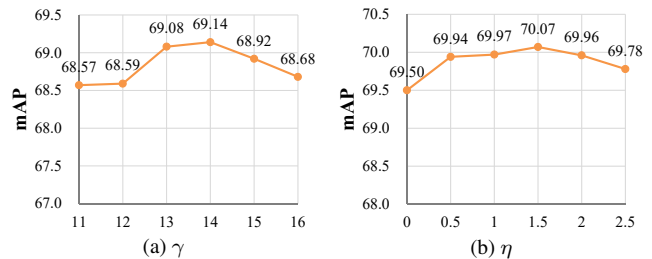


Figure 3. Ablation study about hyperparameters on VOC07 dataset. (a) mAP (%) of baseline with FSR on different  $\gamma$ . (b) mAP (%) of the proposed method on different  $\eta$ .

network, but also by the classification loss indirectly.

## 5. Conclusion

In this paper, we have proposed a novel knowledge distillation scheme, called pixel distillation, to reduce the computational cost of complex image recognition. It simultaneously simplifies the network architecture and reduces the resolution of the input images. Considering that high-resolution feature maps contain much more semantic and visual information, we proposed a novel feature super-resolution module with high-resolution representation transfer learning to implicitly and explicitly improve performance of student network with low-resolution input. We design a novel staged distillation strategy to bridge the proposed cross-resolution learning mechanism with previous knowledge distillation approaches by introducing an assistant network between the classical teacher-student framework. Experimental results demonstrate that the proposed method can improve the performance of models with compact network architecture and low-resolution input. In the future, we will apply the proposed pixel distillation scheme to other complex tasks like object detection [12], and medical image segmentation [47], *etc.*

**Limitations.** Although the effectiveness of the propose approach has been verified in various experimental settings,



we find that when both the network architecture type and the input resolution of the teacher model and the student model are different, our method cannot bring obvious performance gains. For such challenging cases, we will elaborate on stronger pixel distillation mechanisms in the future.

## References

- [1] Sungsoo Ahn, Shell Xu Hu, Andreas Damianou, Neil D Lawrence, and Zhenwen Dai. Variational information distillation for knowledge transfer. In *CVPR*, pages 9163–9171, 2019. [2](#)
- [2] Jimmy Ba and Rich Caruana. Do deep nets really need to be deep? In *NIPS*, pages 2654–2662, 2014. [1](#), [2](#)
- [3] Guobin Chen, Wongun Choi, Xiang Yu, Tony Han, and Manmohan Chandraker. Learning efficient object detection models with knowledge distillation. In *NIPS*, pages 742–751, 2017. [2](#), [3](#)
- [4] Liqun Chen, Dong Wang, Zhe Gan, Jingjing Liu, Ricardo Henao, and Lawrence Carin. Wasserstein contrastive representation distillation. In *CVPR*, pages 16296–16305, 2021. [2](#)
- [5] Pengguang Chen, Shu Liu, Hengshuang Zhao, and Jiaya Jia. Distilling knowledge via knowledge review. In *CVPR*, pages 5008–5017, 2021. [2](#)
- [6] Tianshui Chen, Muxin Xu, Xiaolu Hui, Hefeng Wu, and Liang Lin. Learning semantic-specific graph representation for multi-label image recognition. In *ICCV*, pages 522–531, 2019. [1](#)
- [7] Jang Hyun Cho and Bharath Hariharan. On the efficacy of knowledge distillation. In *CVPR*, pages 4794–4802, 2019. [7](#)
- [8] Jia Deng, Wei Dong, Richard Socher, Li-Jia Li, Kai Li, and Li Fei-Fei. Imagenet: A large-scale hierarchical image database. In *CVPR*, pages 248–255, 2009. [5](#)
- [9] Mark Everingham, Luc Van Gool, Christopher KI Williams, John Winn, and Andrew Zisserman. The pascal visual object classes (voc) challenge. *IJCV*, 88(2):303–338, 2010. [5](#)
- [10] Yushuo Guan, Pengyu Zhao, Bingxuan Wang, Yuanxing Zhang, Cong Yao, Kaigui Bian, and Jian Tang. Differentiable feature aggregation search for knowledge distillation. In *ECCV*, pages 469–484, 2020. [1](#), [2](#)
- [11] Hao Guo, Kang Zheng, Xiaochuan Fan, Hongkai Yu, and Song Wang. Visual attention consistency under image transforms for multi-label image classification. In *CVPR*, pages 729–739, 2019. [5](#)
- [12] Junwei Han, Dingwen Zhang, Gong Cheng, Nian Liu, and Dong Xu. Advanced deep-learning techniques for salient and category-specific object detection: a survey. *IEEE Signal Processing Magazine*, 35(1):84–100, 2018. [8](#)
- [13] Kaiming He, Xiangyu Zhang, Shaoqing Ren, and Jian Sun. Deep residual learning for image recognition. In *CVPR*, pages 770–778, 2016. [6](#)
- [14] Byeongho Heo, Jeesoo Kim, Sangdoon Yun, Hyojin Park, Nojun Kwak, and Jin Young Choi. A comprehensive overhaul of feature distillation. In *ICCV*, pages 1921–1930, 2019. [2](#)
- [15] Byeongho Heo, Minsik Lee, Sangdoon Yun, and Jin Young Choi. Knowledge transfer via distillation of activation boundaries formed by hidden neurons. In *AAAI*, volume 33, pages 3779–3787, 2019. [2](#)
- [16] Geoffrey Hinton, Oriol Vinyals, and Jeff Dean. Distilling the knowledge in a neural network. In *NIPS*, 2015. [1](#), [2](#), [6](#), [7](#), [8](#)
- [17] Jangho Kim, SeongUk Park, and Nojun Kwak. Paraphrasing complex network: Network compression via factor transfer. In *NIPS*, pages 2760–2769, 2018. [2](#), [4](#)
- [18] Animesh Koratana, Daniel Kang, Peter Bailis, and Matei Zaharia. Lit: Learned intermediate representation training for model compression. In *ICML*, pages 3509–3518, 2019. [2](#)
- [19] Wei-Sheng Lai, Jia-Bin Huang, Narendra Ahuja, and Ming-Hsuan Yang. Deep laplacian pyramid networks for fast and accurate super-resolution. In *CVPR*, pages 624–632, 2017. [4](#)
- [20] Hei Law and Jia Deng. Cornernet: Detecting objects as paired keypoints. In *ECCV*, pages 734–750, 2018. [1](#)
- [21] Quanquan Li, Shengying Jin, and Junjie Yan. Mimicking very efficient network for object detection. In *CVPR*, pages 6356–6364, 2017. [3](#)
- [22] Bee Lim, Sanghyun Son, Heewon Kim, Seungjun Nah, and Kyoung Mu Lee. Enhanced deep residual networks for single image super-resolution. In *CVPRW*, pages 136–144, 2017. [4](#)
- [23] Hanxiao Liu, Karen Simonyan, and Yiming Yang. Darts: Differentiable architecture search. In *ICLR*, 2019. [2](#)
- [24] Li Liu, Qingle Huang, Sihao Lin, Hongwei Xie, Bing Wang, Xiaojun Chang, and Xiaodan Liang. Exploring inter-channel correlation for diversity-preserved knowledge distillation. In *Proceedings of the IEEE/CVF International Conference on Computer Vision*, pages 8271–8280, 2021. [2](#), [7](#)
- [25] Yufan Liu, Jiajiong Cao, Bing Li, Chunfeng Yuan, Weiming Hu, Yangxi Li, and Yunqiang Duan. Knowledge distillation via instance relationship graph. In *CVPR*, pages 7096–7104, 2019. [3](#)
- [26] Yifan Liu, Ke Chen, Chris Liu, Zengchang Qin, Zhenbo Luo, and Jingdong Wang. Structured knowledge distillation for semantic segmentation. In *CVPR*, pages 2604–2613, 2019. [2](#), [3](#)
- [27] Ningning Ma, Xiangyu Zhang, Hai-Tao Zheng, and Jian Sun. Shufflenet v2: Practical guidelines for efficient cnn architecture design. In *ECCV*, pages 116–131, 2018. [6](#)
- [28] Laurens van der Maaten and Geoffrey Hinton. Visualizing data using t-sne. *JMLR*, 9(Nov):2579–2605, 2008. [3](#)
- [29] Wonpyo Park, Dongju Kim, Yan Lu, and Minsu Cho. Relational knowledge distillation. In *CVPR*, pages 3967–3976, 2019. [1](#), [2](#)
- [30] Nikolaos Passalis and Anastasios Tefas. Learning deep representations with probabilistic knowledge transfer. In *ECCV*, pages 268–284, 2018. [2](#), [3](#)
- [31] Adam Paszke, Sam Gross, Soumith Chintala, Gregory Chanan, Edward Yang, Zachary DeVito, Zeming Lin, Alban Desmaison, Luca Antiga, and Adam Lerer. Automatic differentiation in pytorch. In *NIPS*, 2017. [6](#)
- [32] Sylvestre-Alvise Rebuffi, Alexander Kolesnikov, Georg Sperl, and Christoph H Lampert. icarl: Incremental classifier and representation learning. In *CVPR*, pages 2001–2010, 2017. [5](#)

- [33] Adriana Romero, Nicolas Ballas, Samira Ebrahimi Kahou, Antoine Chassang, Carlo Gatta, and Yoshua Bengio. Fitnets: Hints for thin deep nets. 2015. [1](#), [2](#)
- [34] Yuzhang Shang, Bin Duan, Ziliang Zong, Liqiang Nie, and Yan Yan. Lipschitz continuity guided knowledge distillation. In *ICCV*, pages 10675–10684, 2021. [2](#)
- [35] Suraj Srinivas and Francois Fleuret. Knowledge transfer with jacobian matching. In *ICML*, pages 4723–4731, 2018. [2](#)
- [36] Yonglong Tian, Dilip Krishnan, and Phillip Isola. Contrastive representation distillation. In *ICLR*, 2019. [6](#), [7](#)
- [37] Frederick Tung and Greg Mori. Similarity-preserving knowledge distillation. In *ICCV*, pages 1365–1374, 2019. [1](#), [2](#), [6](#), [7](#)
- [38] Catherine Wah, Steve Branson, Peter Welinder, Pietro Perona, and Serge Belongie. The caltech-ucsd birds-200-2011 dataset. 2011. [5](#)
- [39] Tao Wang, Li Yuan, Xiaopeng Zhang, and Jiashi Feng. Distilling object detectors with fine-grained feature imitation. In *CVPR*, pages 4933–4942, 2019. [3](#)
- [40] Zhouxia Wang, Tianshui Chen, Guanbin Li, Ruijia Xu, and Liang Lin. Multi-label image recognition by recurrently discovering attentional regions. In *2017 IEEE International Conference on Computer Vision (ICCV)*, pages 464–472. IEEE, 2017. [5](#)
- [41] Yi Wei, Xinyu Pan, Hongwei Qin, Wanli Ouyang, and Junjie Yan. Quantization mimic: Towards very tiny cnn for object detection. In *ECCV*, pages 267–283, 2018. [3](#)
- [42] Junho Yim, Donggyu Joo, Jihoon Bae, and Junmo Kim. A gift from knowledge distillation: Fast optimization, network minimization and transfer learning. In *CVPR*, pages 4133–4141, 2017. [2](#)
- [43] Lu Yu, Vacit Oguz Yazici, Xialei Liu, Joost van de Weijer, Yongmei Cheng, and Arnau Ramisa. Learning metrics from teachers: Compact networks for image embedding. In *CVPR*, pages 2907–2916, 2019. [2](#)
- [44] Kaiyu Yue, Jiangfan Deng, and Feng Zhou. Matching guided distillation. In *ECCV*, pages 312–328, 2020. [2](#)
- [45] Sergey Zagoruyko and Nikos Komodakis. Wide residual networks. In *BMVC*, pages 87.1–87.12, 2016. [6](#)
- [46] Sergey Zagoruyko and Nikos Komodakis. Paying more attention to attention: Improving the performance of convolutional neural networks via attention transfer. In *ICLR*, 2017. [1](#), [4](#), [6](#), [7](#)
- [47] Dingwen Zhang, Guohai Huang, Qiang Zhang, Jungong Han, Junwei Han, Yizhou Wang, and Yizhou Yu. Exploring task structure for brain tumor segmentation from multi-modality mr images. *IEEE Transactions on Image Processing*, 29:9032–9043, 2020. [8](#)
- [48] Linfeng Zhang, Yukang Shi, Zuoqiang Shi, Kaisheng Ma, and Chenglong Bao. Task-oriented feature distillation. *NIPS*, 33, 2020. [2](#)
- [49] Xiangyu Zhang, Xinyu Zhou, Mengxiao Lin, and Jian Sun. Shufflenet: An extremely efficient convolutional neural network for mobile devices. In *CVPR*, pages 6848–6856, 2018. [5](#), [11](#)
- [50] Sixiao Zheng, Jiachen Lu, Hengshuang Zhao, Xiatian Zhu, Zekun Luo, Yabiao Wang, Yanwei Fu, Jianfeng Feng, Tao Xiang, Philip HS Torr, et al. Rethinking semantic segmentation from a sequence-to-sequence perspective with transformers. In *CVPR*, pages 6881–6890, 2021. [1](#)
- [51] Bolei Zhou, Aditya Khosla, Agata Lapedriza, Aude Oliva, and Antonio Torralba. Learning deep features for discriminative localization. In *CVPR*, pages 2921–2929, 2016. [5](#)
- [52] Feng Zhu, Hongsheng Li, Wanli Ouyang, Nenghai Yu, and Xiaogang Wang. Learning spatial regularization with image-level supervisions for multi-label image classification. In *2017 IEEE Conference on Computer Vision and Pattern Recognition (CVPR)*, pages 2027–2036. IEEE, 2017. [5](#)
- [53] Jinguo Zhu, Shixiang Tang, Dapeng Chen, Shijie Yu, Yakun Liu, Mingzhe Rong, Aijun Yang, and Xiaohua Wang. Complementary relation contrastive distillation. In *CVPR*, pages 9260–9269, 2021. [2](#)

## A. Efficiency of FSR

The proposed FSR will introduce extra computational cost and parameters. In this paper, we use group convolution/deconvolution to reduce the computational cost and number of parameters caused by FSR module, and introduce channel shuffle [49] to maintain the performance. In Table 7, we conduct experiments on two teacher-student pairs, *i.e.*, (b) and (d), to demonstrate how the different number of groups affect the computational cost and performance. The down-sampling rate is set as 4 for all experiments. We can get the following conclusion: 1) Higher groups number would greatly reduce the computational cost and parameters of the FSR module. Especially, for the lightweight network ShuffleNetV2 0.5 in (d), FLOPs will be 126.6 times of the original model when group convolution/deconvolution are not used (3088.30 vs. 24.39). 2) There is no regular relationship between the number of groups and the performance, higher groups number does not always lead to lower performance. Moreover, the performance fluctuation is less than one point for both two teacher-student pairs. This circumstance demonstrates that when the proposed assistant has the same network architecture as the student, the kernel functions required for super-resolution between different channels of features can be very similar. In this paper, in order to achieve a balance between performance and computation, we set 32 groups for the ResNet variants and 1024 groups for the ShuffleNetV2 variants.

Table 7. Efficiency analysis of FSR on VOC07. We report the parameters (M) and FLOPs (M).

	Groups	(b)			(d)		
		Params	FLOPs	mAP	Params	FLOPs	mAP
w/o FSR	-	11.69	259.83	-	2.28	24.39	-
w FSR	1	24.80	1026.32	68.40	54.71	3088.30	58.89
	2	18.24	643.59	69.05	28.50	1557.38	58.25
	4	14.97	452.23	68.80	15.39	791.92	58.14
	8	13.33	356.54	68.86	8.83	409.19	57.76
	16	12.51	308.70	68.47	5.56	217.82	57.56
	32	12.10	284.78	69.14	3.92	122.14	56.99
	64	11.90	272.82	68.75	3.10	74.30	57.50
	128	11.79	266.84	68.84	2.69	50.38	57.48
	256	11.74	263.85	68.57	2.49	38.42	58.73
	512	11.72	262.36	68.43	2.38	32.44	58.38
	1024	-	-	-	2.33	29.45	58.51

## B. Training process of TAS framework

In this section, we provide Algorithm 1 to make the training process of the proposed teacher-assistant-student more clear.

**Algorithm 1:** Training process of TAS framework.

---

**Input:** High-resolution images  $\mathcal{I}_{hr}$ ; low-resolution images  $\mathcal{I}_{lr}$ ;  
teacher network  $f_t(\mathbf{W}_t, \cdot)$ ;

**Output:** Assistant network  $f_a(\mathbf{W}_a, \cdot)$ ; Student network  $f_s(\mathbf{W}_s, \cdot)$ ; FSR module  $f_{fsr}(\mathbf{W}_{fsr}, \cdot)$ ;

- 1 Initialize  $f_s(\mathbf{W}_s, \cdot)$  and  $f_a(\mathbf{W}_a, \cdot)$ ;
- 2 **for**  $i$  in  $1 \dots N$  **do**
- 3     Evaluate  $I_{hr}^i$  by  $f_t(\mathbf{W}_t, \cdot)$ , get  $\mathbf{x}_t$  and  $\mathcal{F}_t$ .
- 4     Feed  $I_{hr}^i$  to  $f_a(\mathbf{W}_a, \cdot)$ , get  $\mathbf{x}_a, \mathcal{F}_a$ .
- 5     **if use prediction distillation then**
- 6          $\mathcal{L}_a = \mathcal{L}_{pkd}(\mathbf{x}_t, \mathbf{x}_a)$ .
- 7     **else if use feature distillation then**
- 8          $\mathcal{L}_a = \mathcal{L}_{fkcd}(\mathcal{F}_t, \mathcal{F}_a, \mathbf{x}_a)$ .
- 9     Optimize  $f_a(\mathbf{W}_a, \cdot)$  via  $\mathcal{L}_a$ .
- 10     Feed  $I_{hr}^i$  to  $f_a(\mathbf{W}_a, \cdot)$ , get  $\mathbf{x}_s^{im}$  and  $\mathcal{F}_s^{im}$ .
- 11      $\mathcal{L}_s^{im} = \mathcal{L}_{pkd}(\mathbf{x}_t, \mathbf{x}_s^{im}) + \eta \mathcal{L}_{hrt}(\mathcal{F}_a, \mathcal{F}_s^{im})$ .
- 12     Feed  $I_{lr}^i$  to  $f_s(\mathbf{W}_s, \cdot)$ , get  $\mathbf{x}_s^{ex}$  and  $\mathcal{F}_{lr}$ .
- 13     Feed  $\mathcal{F}_{lr}(M)$  to  $f_{fsr}(\mathbf{W}_{fsr}, \cdot)$ , get  $\widehat{\mathbf{F}}_{hr}(M)$ .
- 14      $\mathcal{L}_s^{ex} = \mathcal{L}_{pkd}(\mathbf{x}_t, \mathbf{x}_s^{ex}) + \gamma \mathcal{L}_{fsr}(\mathcal{F}_a(M), \widehat{\mathbf{F}}_{hr}(M))$ .
- 15      $\mathcal{L}_s = \mathcal{L}_s^{im} + \mathcal{L}_s^{ex}$ .
- 16     Optimize  $f_s(\mathbf{W}_s, \cdot)$  and  $f_{fsr}(\mathbf{W}_{fsr}, \cdot)$  via  $\mathcal{L}_s$ .

---